Brain Stimulation 14 (2021) 825–836

Contents lists available at ScienceDirect

Brain Stimulation

journal homepage: http://www.journals.elsevier.com/brain-stimulation

Generating artificial sensations with spinal cord stimulation in primates and rodents

Amol P. Yadav [a, b, *], Shuangyan Li [e, m, n], Max O. Krucoff [j, k], Mikhail A. Lebedev [d, l], Muhammad M. Abd-El-Barr [c], Miguel A.L. Nicolelis [c, d, e, f, g, h, i]

[a] Department of Neurological Surgery, Indiana University School of Medicine, Indianapolis, IN, 46202, USA
[b] Paul and Carole Stark Neurosciences Research Institute, Indiana University School of Medicine, Indianapolis, IN, 46202, USA
[c] Department of Neurosurgery, Duke University, Durham, NC, 27710, USA
[d] Center for Neuroengineering, Duke University, Durham, NC, 27710, USA
[e] Department of Neurobiology, Duke University, Durham, NC, 27710, USA
[f] Department of Biomedical Engineering, Duke University, Durham, NC, 27710, USA
[g] Department of Psychology and Neuroscience, Duke University, Durham, NC, 27710, USA
[h] Department of Neurology, Duke University, Durham, NC, 27710, USA
[i] Edmond and Lily Safra International Institute of Neuroscience, Natal, 59066060, Brazil
[j] Department of Neurosurgery, Medical College of Wisconsin & Froedtert Health, Wauwatosa, WI, 53226, USA
[k] Department of Biomedical Engineering, Marquette University & Medical College of Wisconsin, Milwaukee, WI, 53233, USA
[l] Skolkovo Institute of Science and Technology, 30 Bolshoy Bulvar, Moscow, 143026, Russia
[m] State Key Laboratory of Reliability and Intelligence of Electrical Equipment, School of Electrical Engineering, Tianjin, 300130, PR China
[n] Tianjin Key Laboratory Bioelectromagnetic Technology and Intelligent Health, Hebei University of Technology, Tianjin, 300130, PR China

ARTICLE INFO

Article history:
Received 24 December 2020
Received in revised form
1 April 2021
Accepted 30 April 2021
Available online 18 May 2021

Keywords:
Spinal cord stimulation
Neuroprosthetics
Somatosensation
Artificial sensory feedback
Non-human primates

ABSTRACT

For patients who have lost sensory function due to a neurological injury such as spinal cord injury (SCI), stroke, or amputation, spinal cord stimulation (SCS) may provide a mechanism for restoring somatic sensations via an intuitive, non-visual pathway. Inspired by this vision, here we trained rhesus monkeys and rats to detect and discriminate patterns of epidural SCS. Thereafter, we constructed psychometric curves describing the relationship between different SCS parameters and the animal's ability to detect SCS and/or changes in its characteristics. We found that the stimulus detection threshold decreased with higher frequency, longer pulse-width, and increasing duration of SCS. Moreover, we found that monkeys were able to discriminate temporally- and spatially-varying patterns (i.e. variations in frequency and location) of SCS delivered through multiple electrodes. Additionally, sensory discrimination of SCS-induced sensations in rats obeyed Weber's law of just-noticeable differences. These findings suggest that by varying SCS intensity, temporal pattern, and location different sensory experiences can be evoked. As such, we posit that SCS can provide intuitive sensory feedback in neuroprosthetic devices.

Introduction

Lack of sensory feedback from a brain-controlled actuator or prosthetic device is a major hindrance to successful integration of the neuroprosthesis in activities of daily life and rehabilitative protocols [1–3]. The somatosensory cortex (S1) and thalamus have been proposed as potential targets for neurostimulation that could produce naturalistic somatosensory percepts [4–10]. However, stimulating these brain areas requires surgical implantation of deep intracranial electrodes – a procedure associated with significant risks. While peripheral nerve stimulation provides a less invasive alternative, sensations evoked with this method are highly localized, and thus limited in their applicability as a general-purpose sensory input pathway to the brain [11–13]. Previously, in a proof-of-concept study it was demonstrated that electrical stimulation of the dorsal surface of the spinal cord can be used to transmit sensory information between multiple rodent brains [14]. Building on this previous work, here we explored whether nonhuman primates can learn to detect and discriminate artificial sensations generated with dorsal thoracic epidural spinal cord

* Corresponding author. Department of Neurological Surgery, Indiana University School of Medicine, Indianapolis, IN, 46202, USA.
E-mail address: apyadav@iu.edu (A.P. Yadav).

https://doi.org/10.1016/j.brs.2021.04.024

stimulation (SCS). To understand the relationship between SCS parameters and sensory detection – which is critical for the development of novel neuroprosthetic devices – we performed a robust psychophysical evaluation of the animals' ability to detect sensations while SCS parameters were altered. We also examined how sensory discrimination changes when SCS parameters are varied in both rodent and primate models, and we asked whether animals can learn to discriminate sensations generated by SCS patterns that vary in frequency and spatial location. After training the animals to discriminate SCS patterns, we determined whether artificial sensations evoked by SCS of variable frequency follow Weber's law of just-noticeable differences (JND) - a critical property defining sensory discrimination.

Results

We implanted three rhesus monkeys with percutaneous epidural SCS electrodes at the dorsal thoracic spinal level and trained them to perform a two-alternative forced choice task (2AFC) using a joystick-controlled cursor (Fig. 1a, Supplementary Figure 1). In a typical experimental session, a monkey was seated in a chair in front of a monitor that displayed task-related cues. The animals moved a hand-held joystick to control a cursor on a screen (Fig. 1b).

A typical trial consisted of a brief 1 s center hold period after which two targets appeared. After a brief preparatory period of 100–1000 ms during which a trial cue was presented, the monkeys had to move the cursor into one of the targets to obtain a juice reward. Monkeys were initially trained to identify the correct target using a visual cue; however, during the experimental sessions, no visual cues were presented, and they selected a target by interpreting SCS cues alone. In the detection task, monkeys had to select the left target if SCS was delivered during the preparatory period and right target if no SCS was delivered (Fig. 1c). In the discrimination task, monkeys had to select the left target for the 100 Hz stimuli and right target for the 200 Hz stimuli (frequency discrimination) and the left target for electrode pair 1 and right target for electrode pair 2 (spatial discrimination).

Monkeys learned to detect SCS stimuli

Monkeys M, O, and K learned to detect SCS-induced sensory percepts evoked using percutaneous dorsal thoracic epidural electrodes (T7 for monkey M, T5-T6 for monkey O, T5-T6 for monkey K). Performance of all monkeys started below chance levels of 50% and reached above 90% after learning (Fig. 2a). Monkey M started detection performance at 49% and reached a maximum of 93% in 16 days; monkey O started at 49% and reached a maximum of 97% in 10 days; and monkey K started at 41% and reached a maximum of 90% in 8 days.

Electrode thresholds and electrode mapping

Once the monkeys learned to detect SCS sensations, we used psychometric analysis to determine the detection thresholds for different electrode combinations (Fig. 2b). We observed that the detection thresholds varied from 315.6 μA to 340 μA for monkey O and 197 μA–748 μA for monkey K for different cathode-anode electrode pairs (Fig. 2c, right). Once electrode thresholds were determined, we mapped the bipolar electrode pairs to locations on the monkey's body by stimulating at suprathreshold amplitudes and observing stimulation-induced minor muscle twitches or skin flutter. We observed that muscle twitches/skin flutter were elicited in the trunk and abdomen area only at suprathreshold values but not at sensory threshold values (Fig. 2c). We also noted that in both monkeys K and O experimentally determined sensory thresholds were always lower than the observed motor thresholds for each cathode-anode electrode pair (Supplementary Figure 3b).

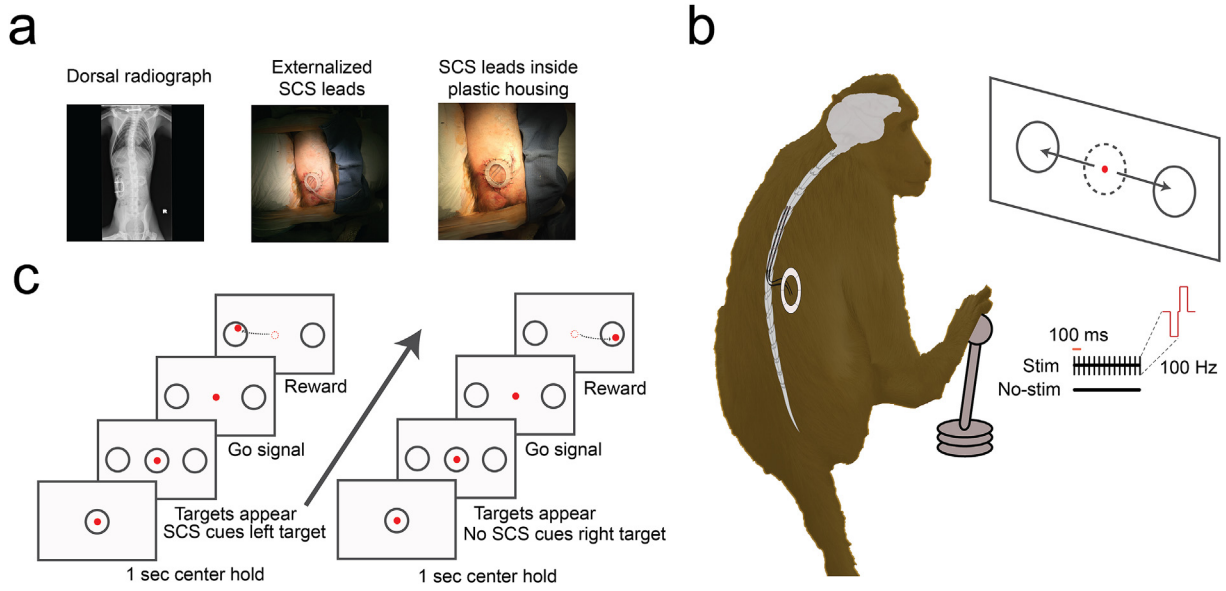

Fig. 1. Surgery and experimental task setup. a) We implanted three non-human primates (rhesus monkeys) with SCS percutaneous leads over the T6-T10 dorsal epidural surface of the spinal cord. Leads were externalized from the lower back area and secured inside a custom plastic housing. Leads were manually accessed by the experimenter for daily training and connected to a custom pulse stimulator. b) Monkeys were seated in a primate chair in front of a computer monitor with access to a hand-controlled joystick. They participated in a two-alternative forced choice task (2AFC) by moving the joystick controlling a cursor on the screen in order to receive a juice reward. c) On each trial, monkeys had to hold the cursor inside the center circle for 1 s. After that, targets appeared on the left and right side of the center. Monkeys were presented with 'SCS-ON' (biphasic, 100 Hz, 200 μs, 1 s) cue or 'SCS-OFF' cue when the targets appeared. After a brief, variable hold period (100–1000 ms), the center circle disappeared which indicated them to move the joystick. Monkeys had to move the cursor inside the left target on 'SCS-ON' trials and inside the right target on 'SCS-OFF' trials. Correct response resulted in juice reward. In the SCS discrimination task, stimulation was delivered at 200 μs for 1 s. Monkeys had to select left target for 100 Hz stimulus and right target for 200 Hz stimulus in the frequency discrimination task. For spatial discrimination task, monkeys had to choose left target when stimulation was delivered at electrode pair 1 and right target for stimulation at electrode pair 2.

Sensitivity to detection of sensory percepts in primates

Thereafter, we investigated the psychophysical relationship between stimulation parameters and detection of sensory percepts by varying stimulation amplitudes along with stimulation frequency, pulse-width, or duration of stimulation while keeping the other two parameters constant.

We varied amplitude from 50 μA to 800 μA for pulse-widths of 50 μs, 100 μs, 200 μs, and 400 μs for monkey K, and pulse-widths of 100 μs, 200 μs, and 400 μs for monkey O. Frequency and duration of stimulation were held constant (Fig. 3a and 3e, and Supplementary Figure 2a). We observed that stimulus detection threshold significantly decreased with increasing stimulation pulse-width ($p < 0.05$, repeated measures one-way ANOVA) for both animals (Fig. 3h).

We varied amplitude from 50 μA to 800 μA for frequencies of 10 Hz, 20 Hz, 50 Hz, 100 Hz, 200 Hz, and 500 Hz for monkey K, and frequencies of 20 Hz, 50 Hz, 100 Hz, 200 Hz, and 500 Hz for monkey O while keeping pulse-width and duration of stimulation constant (Fig. 3b and 3f, and Supplementary Figure 2b). We observed that stimulation detection threshold significantly decreased with increasing stimulation frequency ($p < 0.05$, repeated measures one-way ANOVA) for both animals (Fig. 3i).

We varied amplitude from 50 μA to 600 μA for duration of 50 ms, 100 ms, 500 ms, and 1000 ms for monkey K, and amplitude between 50 μA and 700 μA for duration of 50 ms, 100 ms, and 500 ms for monkey O, while keeping pulse-width and frequency of stimulation constant (Fig. 3c and 3g, and Supplementary Figure 2c). We observed that stimulation detection threshold significantly decreased with increasing stimulation duration ($p < 0.05$, repeated measures one-way ANOVA) for both animals (Fig. 3j).

In monkey K, we varied both frequency and duration of stimulation while keeping amplitude and pulse-width of stimulation constant. We observed that as the frequency of stimulation increased, the duration of stimulation to reach detection threshold decreased (Fig. 3d and 3k). Monkey K was able to detect a sensory percept generated by merely two stimulation pulses delivered at 1000 Hz.

Sensitivity to detection of sensory percepts in rats

In a proof-of-principle study, we previously showed that rats learn to detect sensations generated by SCS delivered at T2 spinal level [14]. In order to study the psychophysical performance of rats pertaining to sensory detection, initially we trained rats to detect

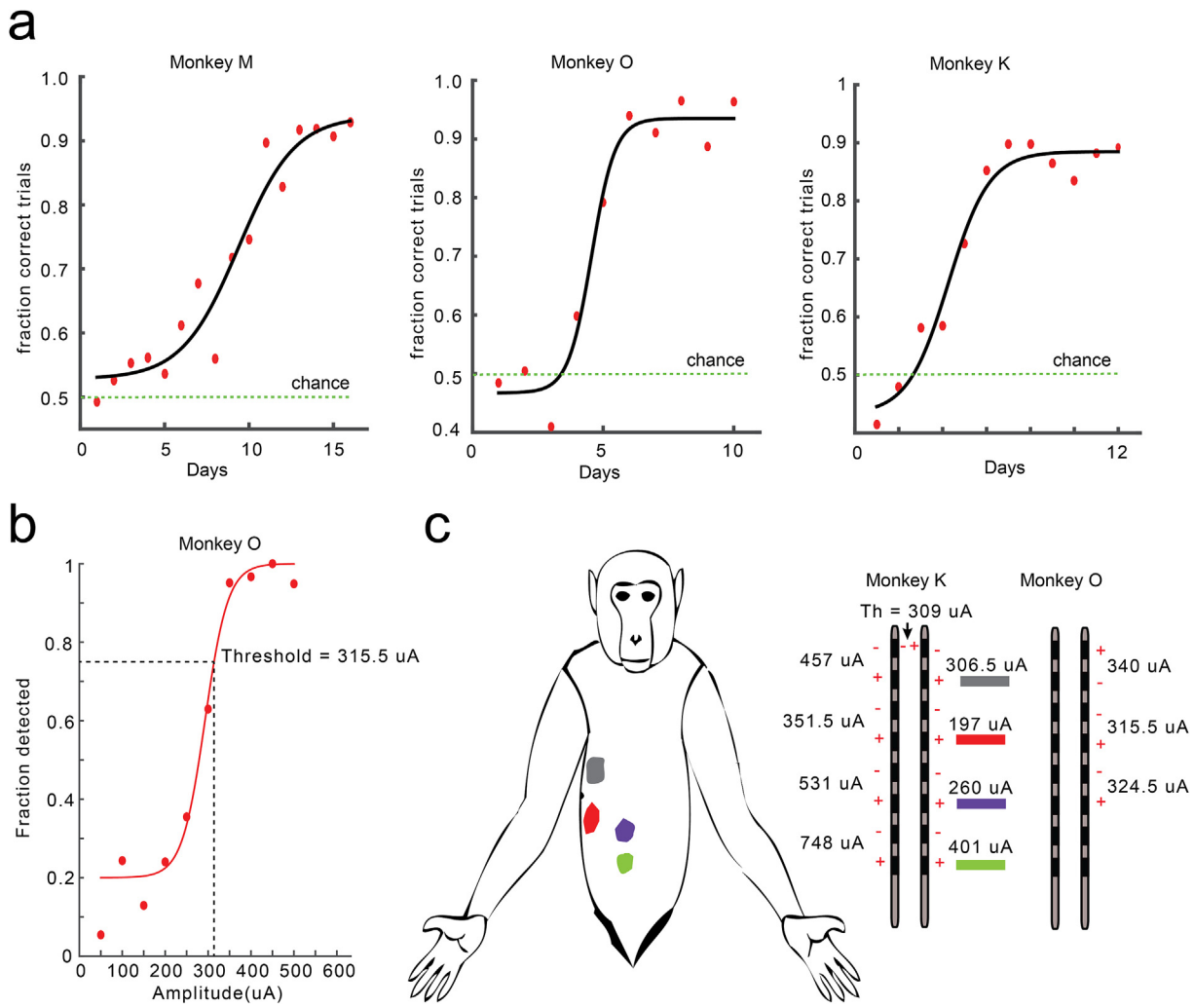

Fig. 2. Monkeys learned to detect SCS stimuli. a) Learning curves (sigmoidal fits) for monkeys M, O, and K showing behavioral performance (fraction correct trials) as a function of training days. b) Psychometric function showing fraction trials detected as a function of stimulation amplitude in monkey O. Detection threshold is defined as amplitude at which monkeys achieved 75% performance on detection task. c) Mapping of bipolar electrode pairs (as indicated by pairs of±signs) on monkey K's body where stimulation on right-side electrode at suprathreshold amplitude elicited minor muscle twitches or skin flutter. Mapped area is color coded by electrode pairs and corresponding sensory thresholds shown on right. Monkey body shape is adapted from Ref. [15].

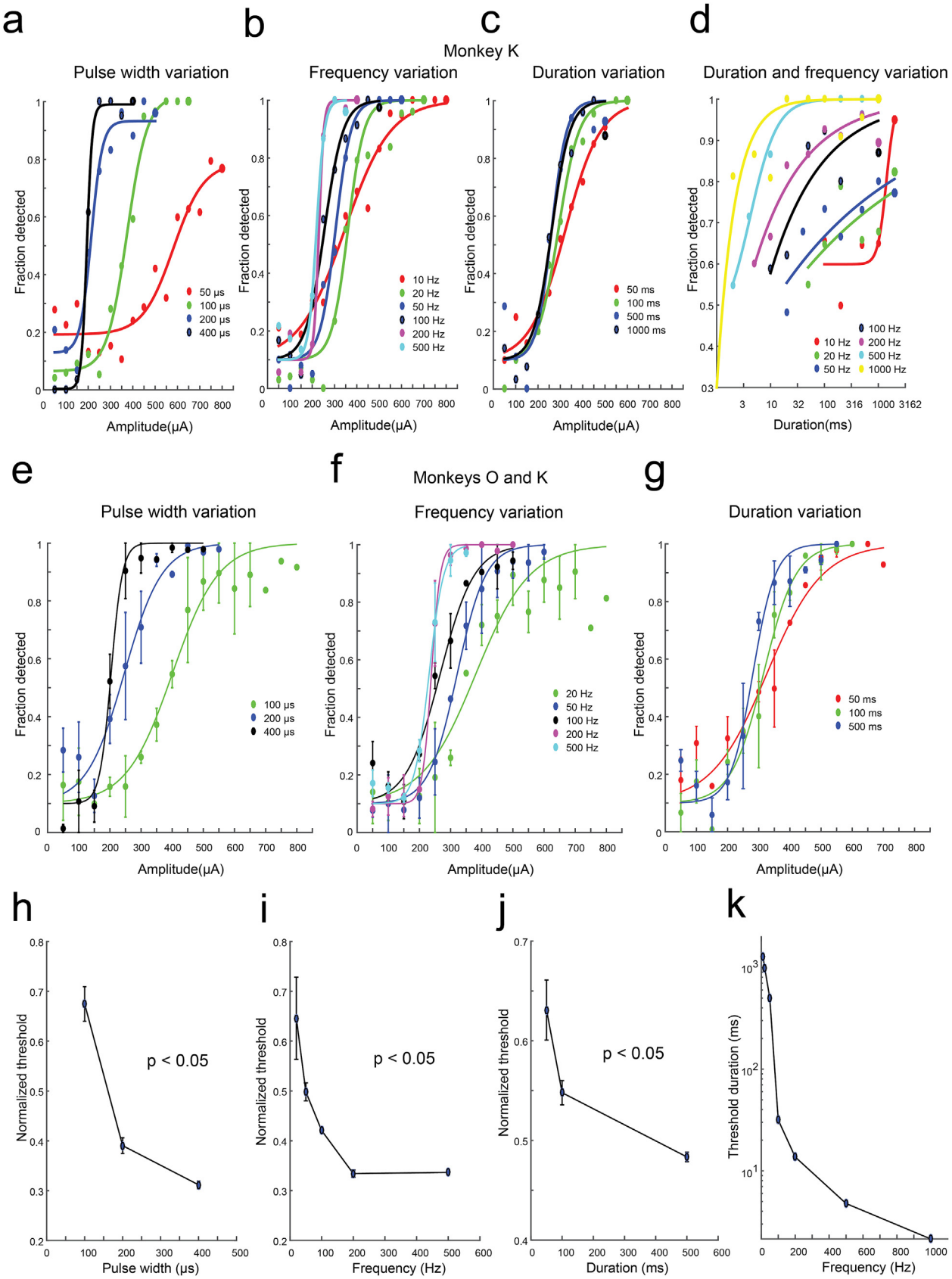

Fig. 3. Psychophysical evaluation of SCS sensory detection with varying stimulation parameters in primates. Once monkeys learned to detect SCS stimuli at the standard parameters (frequency: 100 Hz, pulse width: 200 μs, duration: 1 s), we allocated different blocks of sessions where (pulse width & amplitude; panels 'a' and 'e'); (frequency & amplitude; panels 'b' and 'f'); and (duration & amplitude; panels 'c' and 'g') were varied while keeping other parameters constant. In monkey K, in a separate block, frequency and duration was varied with other parameters constant (pulse width: 200 μsec and amplitude: 325 μA). Psychometric curves in a-g are sigmoidal fits. Panels a–d represent psychometric curves for monkey K, while panels e–g represent psychometric curves fitted to data averaged across monkeys K and O (circles and error bars are mean ± sem). Panels h, i, j, indicate normalized

SCS stimuli using a 2-AFC task in a slightly modified behavioral chamber (Fig. 4a and 4b). We trained five rats to detect SCS stimuli delivered at the T3 spinal level (frequency: 100 Hz, pulse-width: 200 ms, duration: 1 sec, biphasic pulses at 243.7±57.9 mA, Fig. 4c).

Once rats learned the basic detection task, we varied stimulation parameters such as: pulse width (50–400 μs); frequency (10–500 Hz); and duration (50–1000 ms) independently with stimulation amplitude (Fig. 5a, 5d – pulse width; 5b, 5e – frequency; and 5c, 5f – duration). Similar to the results in monkeys, we observed that stimulation detection thresholds significantly decreased with increasing pulse-width (Fig. 5g, $p < 0.0001$, repeated measures one-way ANOVA), frequency (Fig. 5h, $p < 0.0001$, repeated measures one-way ANOVA) and duration (Fig. 5i, $p < 0.05$, repeated measures one-way ANOVA) for all rats.

Sensory discrimination in primates

We then trained monkeys K and O to discriminate SCS that varied in frequency as well as location of stimulation. On frequency discrimination (100 Hz vs 200 Hz, Fig. 6a), monkey O's performance improved from 29% on day 1 to 96% on day 17 of training, while monkey K's performance improved from 74% on day 1to 81% on day 11 (Fig. 6b). Spatial discrimination was achieved by stimulating electrode pair 1 versus electrode pair 2 (Fig. 6c), where monkey O's performance improved from 46% on day 1to 97% on day 11 and monkey K's performance improved from 74% on day 1to 86% on day 7 (Fig. 6d).

Sensory discrimination and Weber's law in rats

In a proof-of-principle study, we had previously shown that rats can learn to discriminate up to four different patterns of stimulation [14]. In our current work, we trained rats to systematically discriminate SCS stimuli with specific frequencies using the same behavioral setup that was used for the detection task (Supplementary Figure 5a). In the basic training, rats learned to discriminate between 10 Hz and 100 Hz of stimulation delivered at pulse-width of 200 μsec, and duration of 1 s (Supplementary Figure 5b). Thereafter, we studied whether discrimination of sensations induced by different stimulation frequencies follows the rules of Weber's law [16], which states that Just-Noticeable Differences (JNDs) between a standard frequency and comparison frequency should linearly increase with the standard frequency of stimulation. To this end, we determined JNDs at different standard frequencies (10–100 Hz) where the comparison frequency was higher than the standard (Fig. 7a). We observed that JNDs had a significant linearly increasing relationship with the standard frequency of stimulation (Fig. 7b, $p < 0.0001$, linear regression test). After that, we kept the standard as a higher frequency value (100–400 Hz) and decreased the comparison frequency randomly from that value (Fig. 7c). In this case also, we observed that the JNDs for lower frequency comparison significantly increased linearly as the standard frequency increased (Fig. 7d, $p < 0.0001$, linear regression test). These results suggest that the JND rule defined by Weber's law holds true for sensory discrimination of SCS frequencies.

Discussion

In this study, we found that rhesus monkeys and rats can learn to detect and discriminate artificial sensations induced by SCS following several days of exposure. The threshold for detecting SCS decreases with increasing pulse width, frequency, and duration of the stimulus. We also documented the ability of monkeys to discriminate sensations that are generated by stimulation pulses with varying frequency and spatial location. In rats, we showed that the just-noticeable differences (JNDs) from a perceivable stimulus frequency were linearly related to the perceivable frequency when it was compared with a stimulus that had either higher or lower frequency. These results demonstrated the unique ability of SCS as a novel transmission channel to the brain to encode highly contextual sensory information.

Our results on behavioral sensitivity to detection of sensation in rodents and primates were comparable to those observed with Intracortical Microstimulation (ICMS) of S1 [5,17]. Notably, sensitivity to stimulus amplitude increased with increasing pulse width, frequency, and duration of stimulation. However, longer pulses needed significantly higher charge to reach threshold in both primates (Supplementary Fig. 4a, 4b, and 4c, $p < 0.05$ – repeated measures one-way ANOVA) and rodents (Supplementary Fig. 4d, 4e, and 4f, $p < 0.0001$ – repeated measures one-way ANOVA), similar to that observed in the ICMS study [5]. ICMS amplitude using currently FDA-approved UTAH arrays is usually restricted below ~100 μA due to the possibility of brain tissue damage, which limits the amplitude range for neuroprosthetic applications between detection thresholds of 20–50 μA and maximum allowable safe amplitude of ~100 μA. In our SCS study, detection thresholds had a wider range from 200 to 800 μA at different stimulation settings and all detection thresholds were consistently on the non-damaging side of the boundary between damaging and non-damaging stimulation delineated by Shannon equation [$\log(D) = k - \log(Q)$, with $k = 1.85$] on log charge density versus log charge per phase plot (Supplementary Figure 3a) [18]. Assuming a commercially accepted maximum charge density of 30 μC/cm^2 and minimum pulse-width of 50 μs [19], it could be estimated that maximum SCS current of ~80 mA in monkeys and ~3 mA in rats could be delivered using electrode contacts (monkeys: 0.1319 cm^2; rats: 0.005 cm^2) reported in our study without causing tissue damage.

Frequency modulation has been historically considered a promising method for providing sensory feedback with several studies showing that animals are capable of discriminating ICMS frequencies and that frequency modulation obeys Weber's law. [4,20–22], While ICMS amplitude modulation in monkeys failed to follow Weber's law [5], experiments in rats showed that modulation of perceived intensity by amplitude and pulse-width modulation followed Weber's law [17]. In our study, we investigated whether rats and monkeys could learn to discriminate SCS frequencies. Although monkeys O and K learned to discriminate 100 Hz SCS from 200 Hz, after taking a closer look at their learning curves it was evident that they displayed different learning behaviors in the frequency discrimination task (Fig. 6b). Monkey O started at lower discrimination performance at earlier training sessions but reached higher level of performance toward the end of training, whereas monkey K's performance started higher than chance and improved marginally as the training progressed. These

detection thresholds (normalized by maximum amplitude used in the experiment block of each individual monkey) averaged across both monkeys (mean ± sem). Detection threshold were calculated as 75% fraction detected at the stimulation parameters shown in panels a–c (monkey K) and Supplementary Fig. 2 a-c (monkey O). P-values were calculated using repeated measures one-way ANOVA. Panel k shows threshold duration obtained as 75% detection from curves in panel d as a function of frequency.

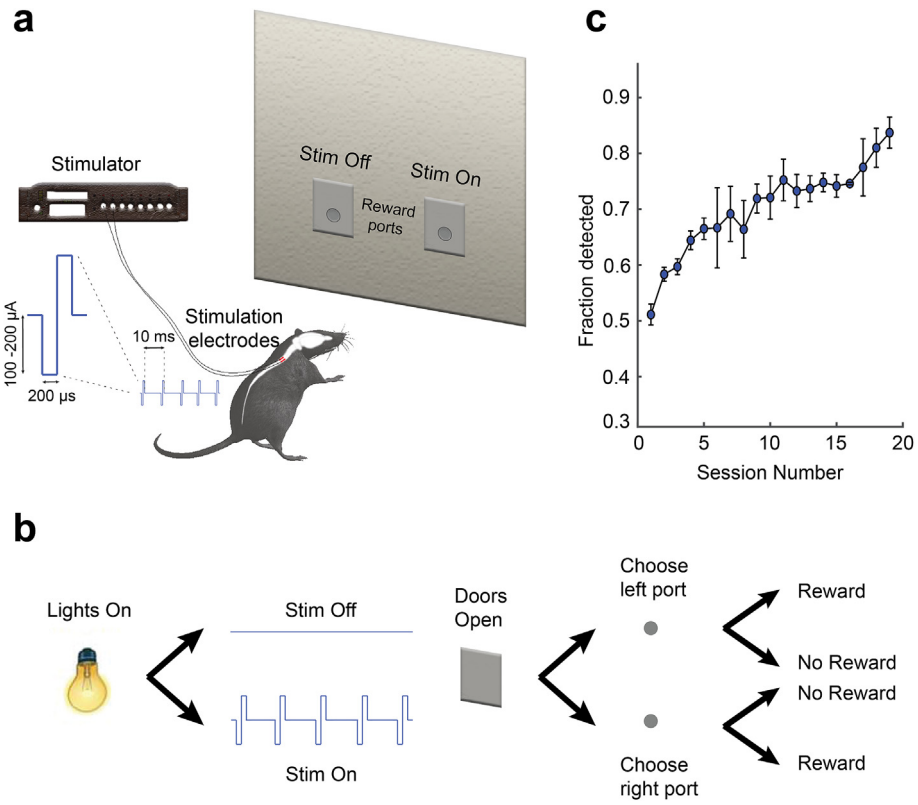

Fig. 4. Behavioral task setup and rats learned to detect SCS stimuli. a) The experiment task consisted of a closed behavioral chamber with two reward ports on one side of the chamber. The ports were covered with vertical sliding doors. Five rats were implanted with bipolar stimulation electrodes on the dorsal surface of the spinal cord at the T3 spinal level. b) Task consisted of a house light turning 'on', followed by sensory cues for 1 s. During the cue period SCS was either delivered or not delivered. After the cue period both reward doors opened, and the rat had to make a nose poke response in either of the ports to receive water reward. If SCS was delivered rats had to poke inside the left port and if not delivered, then they had to poke inside the right reward port. Poking in the correct reward poke initiated a water reward, while incorrect pokes were not rewarded. c) Rats learned to detect SCS stimuli over a period of 15–25 days as indicated – learning curve showing task performance indicated by fraction trials detected as a function of training sessions. Circles and error bars indicate mean ± sem.

differences in learning behavior could be attributed to the fact that monkey O was stimulated at constant amplitude for both frequency values (100 Hz and 200 Hz) while monkey K was stimulated at each frequency's threshold amplitude. It is quite possible that monkey O was discriminating differences in perceived magnitudes of the sensory percepts while monkey K was discriminating differences in the qualitative nature of the percepts induced. Rats are capable of discriminating temporal patterns of SCS when the number of pulses are kept constant but the frequency of stimulus is varied [14]. In addition to that, our current results indicate that JNDs associated with SCS frequency discrimination in rats clearly follow Weber's law because JNDs linearly increased with standard stimulation frequency (Fig. 7b and 7d). It could be surmised from Fig. 7b that there were at least three discriminable percepts between 10 Hz and 200 Hz; first percept at 10 Hz, second percept at 60 Hz because JND at 10 Hz was ~50 Hz; and third percept at 180 Hz since JND at 60 Hz was ~120 Hz. It can be argued that applying frequency modulation simultaneously with amplitude and pulse-width modulation would potentially increase the number of distinct discriminable percepts that are possible within the amplitude range allowed on current SCS electrodes. Therefore, further experiments exploring the relationship between sensory discrimination and frequency, pulse-width, amplitude, and duration of stimulation are necessary to understand how these parameters relate to perceived intensity and quality of sensation evoked by SCS.

A major advantage of SCS is its ability to target multiple dermatomes simultaneously with a single electrode array. In particular, a single, commercially available SCS lead with multiple contacts can evoke sensations in multiple dermatomes simultaneously due to the bilateral sensory representation of the entire lower body in the ascending dorsal column fibers. It is quite apparent from our results that monkeys can learn to discriminate the spatial location of the sensations evoked by SCS (Fig. 6d). This suggests that we can take full advantage of the rostro-caudal somatotopy represented in the dorsal column fibers in combination with spatiotemporal stimulation patterns to electrically induce targeted tactile or proprioceptive sensations in the body. This view is also supported by evidence from computational studies which indicate that epidural SCS activates dorsal column fibers up to a depth of 0.2–0.25 mm from the dorsal surface [23–27]. However, additional work on miniaturizing electrode contacts and accurate medio-lateral/rostro-caudal mapping of SCS-induced sensations needs to be performed to be able to elicit precise sensations. In addition, the ability of SCS to modulate neuronal activity in supraspinal brain structures is quite desirable from a neuroprosthetic as well as a therapeutic application standpoint [14,28–31,34]. A major limitation of our study is the short experimental time (Supplementary Figure 1) we had available for primates – maximum of 5 months – due to the risk of infection associated with externalized SCS leads. A fully implantable stimulation system, like the one implanted in chronic pain patients could potentially extend our study indefinitely and allow us to perform longer experiments in monkeys. Nevertheless, in rodents we were able to perform longer post-implant experiments because the electrodes and their wires were fully enclosed inside the body.

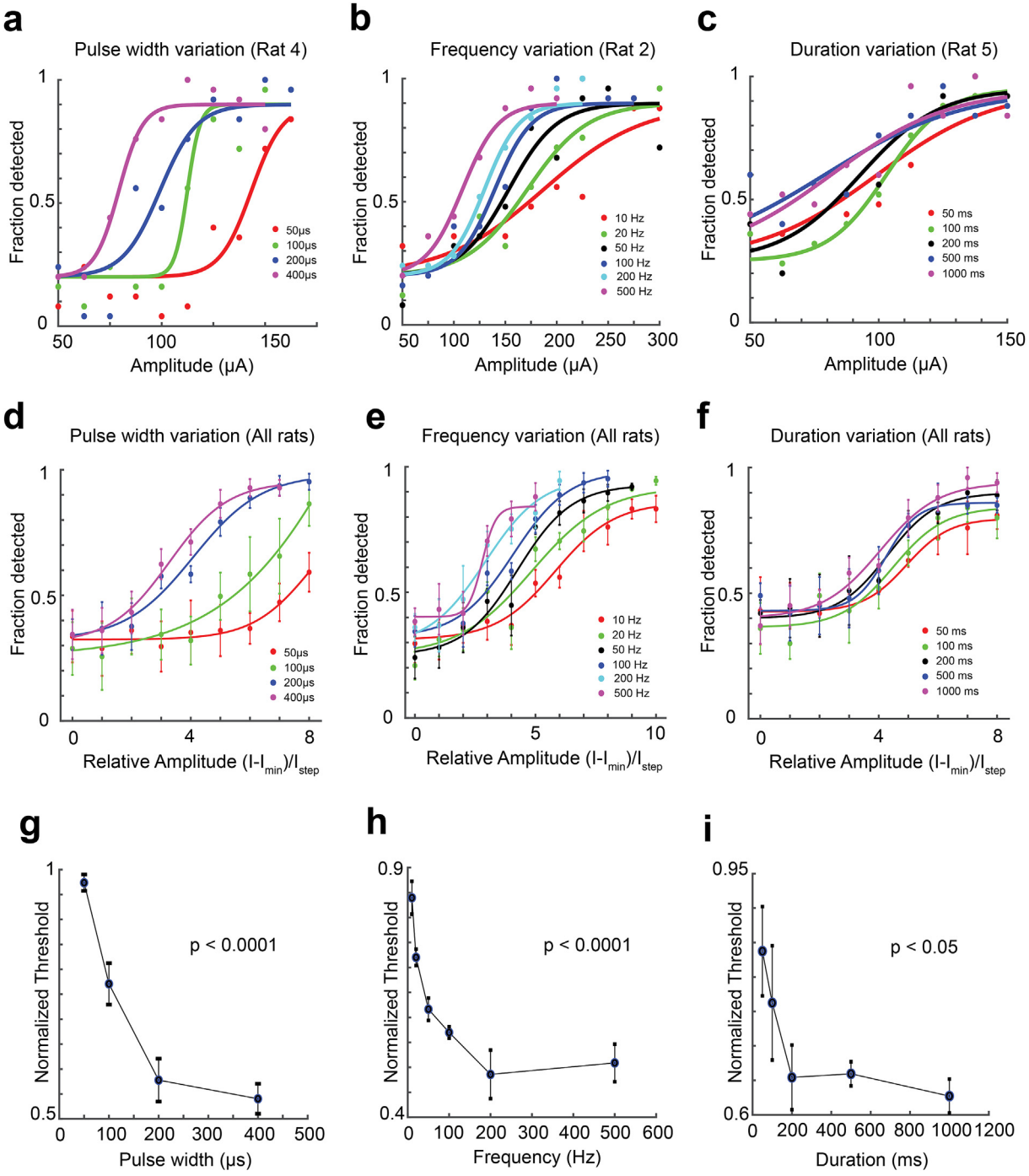

Fig. 5. Psychophysical evaluation of SCS sensory detection with varying stimulation parameters in rats. Once rats learned to detect SCS stimuli at the standard parameters (frequency: 100 Hz, pulse width: 200 μs, duration: 1 s), we allocated different blocks of sessions where (pulse width & amplitude; panel 'a'); (frequency & amplitude; panel 'b'); and (duration & amplitude; panel 'c') were varied while keeping other parameters constant. a, b, c) Psychometric curves from representative rats showing a leftward shift of curves as the pulse-width (rat 4), frequency (rat 2), and duration (rat 5) of stimulation increased. d, e, f) Psychometric curves with averaged data across five rats indicate leftward shift as pulse-width, frequency, and duration are increased. X-axis represents relative amplitude values (for each rat raw amplitude values were subtracted by minimum amplitude and the difference was divided by amplitude step size). Circles and error bars are mean ± sem across five rats. Curves in panels 'a-f' are sigmoidal fits. Panels 'g', 'h', and 'i' indicate normalized detection thresholds. Thresholds were calculated as 75% fraction detected at different stimulation parameters consistent with panels 'a-f' and then normalized by maximum amplitude used in the experimental block of each rat. Circles and error bars are mean ± sem across five rats. P-values were calculated using repeated measures one-way ANOVA.

In conclusion, we have successfully demonstrated that SCS can generate discernible sensory percepts in both rats and monkeys and all together our study strongly shows the potential of SCS to encode sensory information in the brain. Additionally, our behavioral experiments serve as a test bed for future animal studies which could elucidate the neural mechanisms underlying SCS-based sensory detection and discrimination. We envision that SCS can be developed as an artificial sensory feedback channel for delivering targeted tactile and proprioceptive information to the brain.

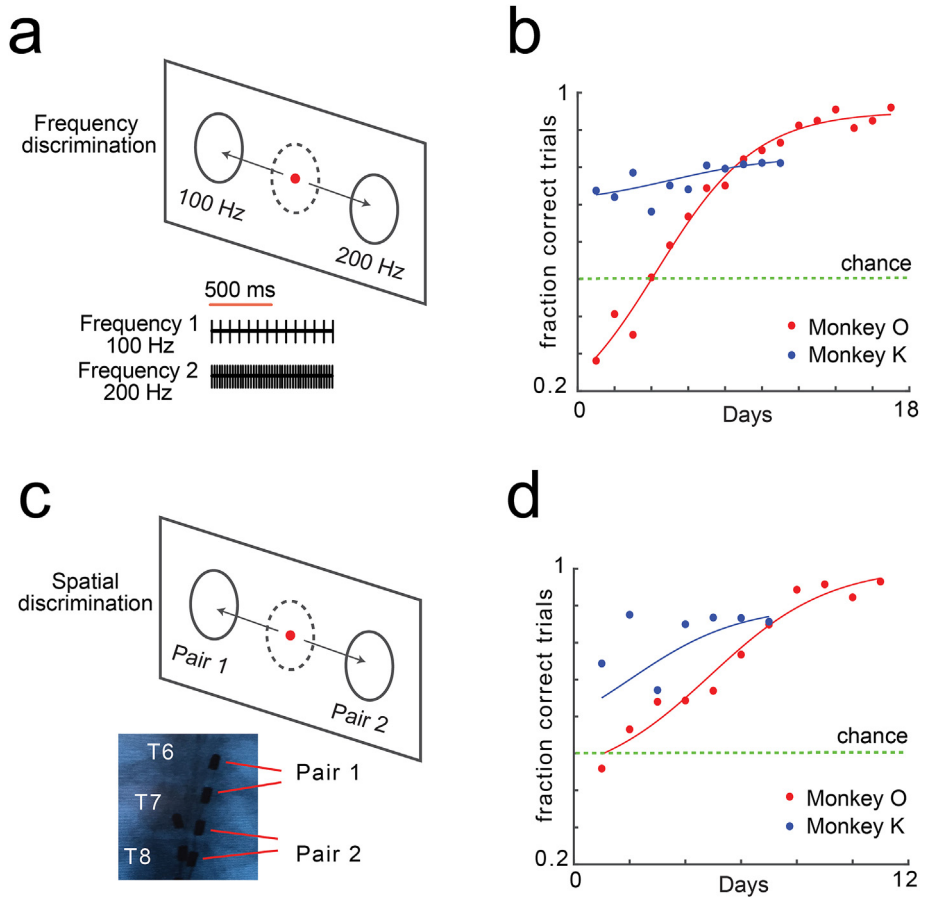

Fig. 6. Monkeys learned to discriminate SCS stimuli varying in frequency and spatial location of electrodes. a,b) Monkeys K and O learned to discriminate SCS stimuli delivered at the same electrode location but varying in frequency (100 Hz vs 200 Hz). Monkey O was stimulated at same amplitude while monkey K was stimulated at the respective threshold amplitude for 100 Hz and 200 Hz. c,d) Monkeys K and O learned to discriminate stimulation delivered at electrode pair 1 (T6 - T7 spinal level) vs electrode pair 2 (T7-T8 spinal level). Curves in panels b and d indicate sigmoidal fits to fraction correct trials displayed as a function of training days.

Methods

All animal procedures were approved by the Duke University Institutional Animal Care and Use Committee and in accordance with National Institute of Health Guide for the Care and Use of Laboratory Animals. Three adult rhesus macaque monkeys (*Macaca mulatta*), monkeys 'M', 'O', and 'K' and five Long Evans rats (300–350 g) participated in the experiments.

Monkey spinal implant surgery

Monkeys M, K, and O were implanted with 8-contact cylindrical percutaneous leads (Model 3186, diameter 1.4 mm, contact length 3 mm, spacing 4 mm, Abbott Laboratories) bilaterally to the spinal mid-line in the dorsal epidural space at T6 – T8 spinal level. Monkey M had two leads with 8 stimulation contacts each, monkey O had two leads, one with 8 contacts (right side) and one with 4 contacts (left side, Model 3146, similar electrode contact dimensions as Model 3186), and monkey K had two leads with 8 stimulation contacts each. Experimental procedures for monkeys M, O, and K lasted approximately 45, 135, and 150 days post-implant after which the leads were explanted (Supplementary Figure 1).

Implant surgery was performed under general anesthesia using standard procedures typical of human implantation (for details see supplementary information and Fig. 1a). Once leads were implanted in the epidural space, a small hole was created in the skin off-midline to externalize the distal end of the lead. Externalized leads were enclosed in a custom plastic cap which was sutured to the skin (Fig. 1a). The plastic cap allowed for access to the leads by the researcher but protection from the animal. The animal wore a protective vest after surgery and throughout the experimental period which prevented its access to the plastic cap sutures to its back.

Monkey SCS detection task

Monkeys were trained to perform a two-alternative forced choice task where they were seated in a chair facing a computer monitor which indicated trial progression (Fig. 1b). On each trial a center target appeared, and the monkey had to move a cursor which was joystick-controlled inside the center target (Fig. 1c). After a brief hold period of 1 s inside the center target, two targets appeared on either side of the center target. Each monkey had to hold the cursor inside the central target for a brief period of 100–1000 ms. During this hold period sensory cues were presented. If SCS was presented (charge-balanced, cathode-first, 200 μs biphasic square pulses at 100 Hz for 1 s using custom microstimulator [32]), then the monkey had to move the cursor to the left target to obtain a juice reward. If SCS was absent, then the monkey had to move the cursor inside the right target. At the end of the hold period, the center target disappeared, thus cuing the monkey

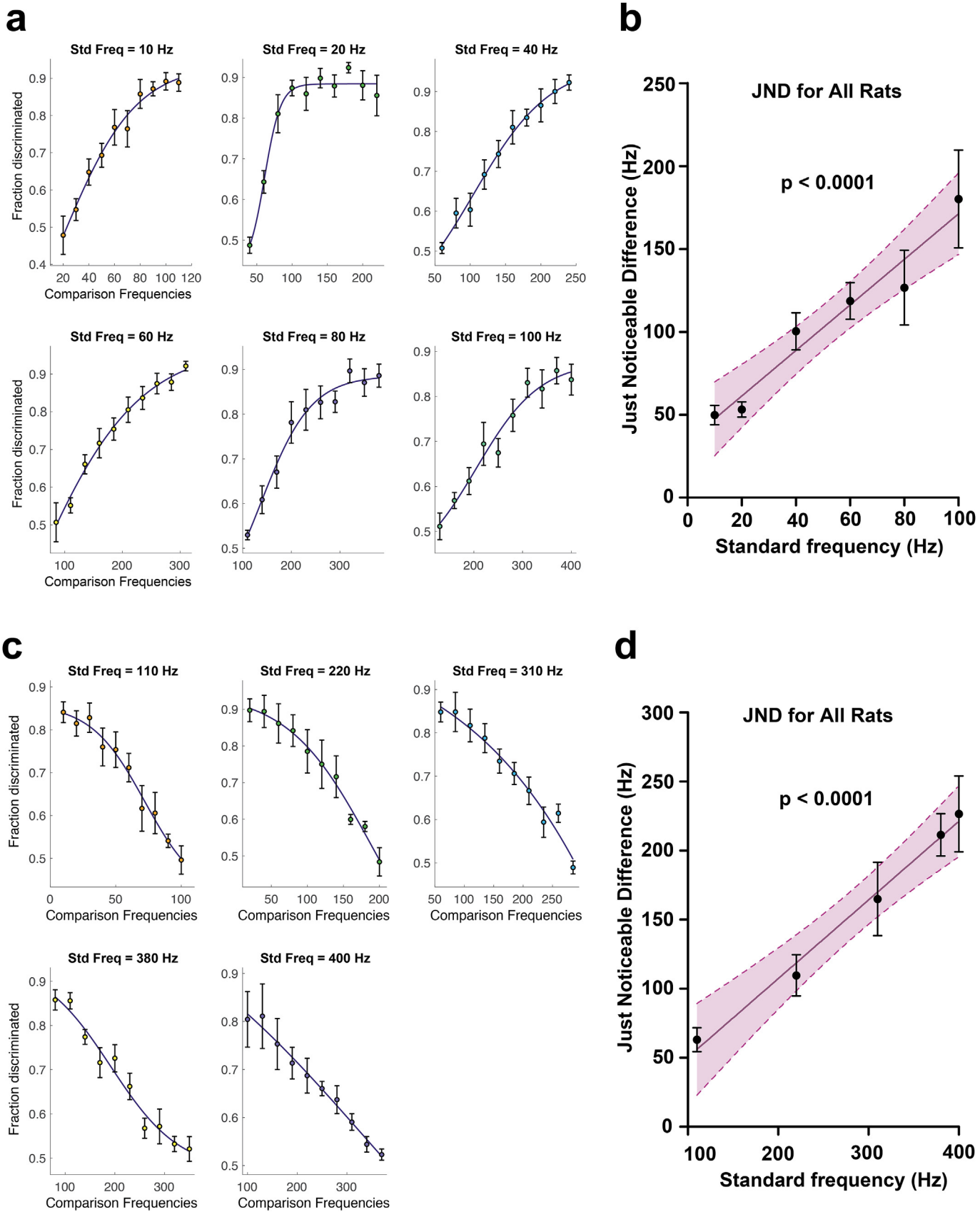

Fig. 7. Discrimination of higher and lower comparison frequency obeys Weber's Law. a) Fraction of trials correctly discriminated from standard frequency of 10 Hz, 20 Hz, 40 Hz, 60 Hz, 80 Hz, and 100 Hz, when compared to a range of higher frequency stimuli. c) Fraction of trials correctly discriminated from standard frequency of 110 Hz, 220 Hz, 310 Hz, 380 Hz, and 400 Hz, when compared to a range of lower frequency stimuli. Circles and error bars in 'a' and 'c' indicate mean ± sem. Curves indicate sigmoid fits to the data. Just-noticeable difference (JND) is considered as the comparison frequency value that achieves 75% discrimination ability. b, d) Just-noticeable difference as a function of standard frequency is indicated by black circles and error bars. Black line is linear regression fit to the data and pink bounds indicate 95% confidence bound of the regression line. JNDs associated with higher frequency and lower frequency comparison were significantly linearly related with standard frequency. P-values were calculated using linear regression test.

to initiate cursor movement toward the reward. Incorrect target reaches were not rewarded. Initiation of movement prior to the end of the hold period terminated the trial without reward and a blank screen was displayed 3 s before starting next trial. The learning performance of monkeys was studied using percentage correct (PC) trials.

Monkey psychometric evaluation of detection thresholds

Once monkeys were trained on the detection task and their performance was above 85%, detection thresholds were determined for different electrode combinations using psychometric testing. Particularly, during 'Stimulation ON' i.e. 'left target rewarded' trials, the stimulation amplitude was randomly varied from 50 μA to a manually determined upper limit which was below the motor threshold. Only left target trials were analyzed and a percentage correct (PC) performance at each stimulation amplitude value was determined. A sigmoid curve was fit to the PC values and 75% was considered as detection threshold. This was repeated for several electrode combinations.

Monkey electrode mapping

In monkey K, once sensory detection thresholds were determined, we mapped the location of electrode pairs to location on the monkey's body by sedating the monkey and stimulating those electrodes above the sensory threshold values. Areas on the body surface that elicited minor muscle twitches or skin flutter were marked (Fig. 2c, left) and the motor thresholds were noted. In monkey O, these observations were not made under sedation but while it was seated in the primate chair.

Monkey detection thresholds as stimulation parameters vary

During sets of consecutive sessions, we varied amplitude and frequency or amplitude and pulse-width or amplitude and duration of stimulation while keeping other parameters constant (for stimulation parameter ranges, see Supplementary Table 1). The standard parameters that remained constant while others were varied were frequency: 100 Hz, pulse width: 200 μsec, and duration: 1 s. In monkey K, we varied frequency (10–1000 Hz) and duration (1–2000 ms) of stimulation simultaneously while keeping pulse width and amplitude constant at 200 μs and 325 μA respectively. Detection thresholds for each monkey were normalized by maximum amplitude used in the experiment block of that monkey before statistical analysis.

Monkey sensory discrimination

In the frequency discrimination task, each monkey was instructed to move the cursor inside the left target for 100 Hz and right target for 200 Hz respectively (Fig. 6a). In the spatial discrimination task, the monkey was instructed to move the cursor inside the left target for electrode pair 1 and inside right target for electrode pair 2 respectively (Fig. 6c).

Rat pre-training and SCS electrode implantation

Moderately water deprived rats were placed inside the behavioral chamber for 2 days to acclimatize to the behavioral environment. The behavioral chamber had two doors on one side of the walls which enclosed water reward ports (Fig. 4a), slightly modified from the one previously described [33]. Rats were gradually trained to receive water reward from the ports. Initially, both reward doors were kept open and rats learned to receive water by licking at the water dispensing spout. Later, the doors were kept closed and would open a few seconds after the house light turned on. In subsequent sessions, left and right doors would open on alternate trials and rats learned to obtain reward from each port alternatively. The pre-surgical training period lasted approximately 8–10 days.

Thereafter custom designed SCS electrodes (1 mm × 0.5 mm contacts arranged transversely in a bipolar configuration with 0.25 mm spacing using a 0.025 mm thickness platinum foil, Goodfellow Cambridge Limited, England) were implanted into the epidural space under T3 vertebra as described in our previous article [29]. After the rats recovered from the spinal surgical procedures, cathode leading stimulation pulse trains were delivered at the SCS electrodes using a multi-channel constant current stimulator (Master-8, A.M.P.I, Jerusalem, Israel) at stimulation settings which were determined depending on the behavioral task under consideration (Fig. 4a).

Rat sensory detection task

After recovery from surgery, rats were introduced to a two-alternative forced choice task (2AFC) to learn detection of SCS stimuli in the chamber (Fig. 4b). At the beginning of each trial, a light in the chamber was turned on for 1 s as a reminder for the animals to pay attention. After the light turned off, the rats received a sensory cue for 1 s. The sensory cue either consisted of cathode-leading bipolar square pulse trains (pulse width: 200 μs, Frequency: 100 Hz, duration: 1 s) or no stimulation pulses (interval: 1 s) at each trial. After a brief delay of 0.5 s both reward doors opened, and rats had to respond by choosing the left door for 'SCS ON' trials and right door for 'SCS OFF' trials. Incorrect responses were not rewarded. During the learning of this basic detection task, the intensity of the delivered current was determined before each session and set using procedures described before [14,29,31] (mean ± std, intensity at 100 Hz was 243.7 ±57.9 μA).

Rat sensory detection psychophysics

Once rats learned the basic sensory detection task and their performance was above 80%, stimulation parameters were varied in a systematic manner during the SCS-ON trials. In different experimental sessions, stimulation parameters such as frequency and amplitude, pulse-width and amplitude, and pulse train duration and amplitude were varied while other parameters were kept constant (standard parameters: pulse width: 200 μs; Frequency: 100 Hz; duration: 1 s), and sensory detection threshold amplitude was determined (for stimulation parameter ranges see Supplementary Table 1). For all the conditions, the detectable level of the amplitude was defined as 75% accuracy of behavioral performance. Detection thresholds for each rat were normalized by maximum amplitude used in the experiment block of that rat before statistical analysis.

Rat sensory discrimination task

In a 2AFC task, rats were presented with either a low frequency stimulus or a high frequency stimulus during the sensory cue period in the behavioral chamber. For either frequency, the stimulus was delivered at the same amplitude (determined at each session), pulse width (200 μs), and duration (1 s). After a brief delay period following sensory cue presentation, rats had to choose the left door for higher frequency stimulus and right door for lower frequency stimulus to obtain reward (Fig. 4a). Initially, rats were trained to discriminate between 10 Hz and 100 Hz frequency. Incorrect trails were not rewarded.

Weber's law and sensory discrimination

Once rats learned to discriminate 10 Hz stimulus from 100 Hz stimulus, demonstrated by consistent discrimination performance above 80%, the lower frequency (standard frequency) was kept constant during right door trials while the higher frequency (comparison frequency) was randomized between 20 Hz and 110 Hz during left door trials. Sensory discrimination performance between a standard frequency and comparison frequency was determined as the fraction of trials successfully discriminated for that particular standard and comparison pair. Thus, fraction trials discriminated was plotted as a function of comparison frequency to obtain Just-Noticeable Differences (JNDs) determined as 75% value on the curve. The same experiment was repeated for different standard frequency values such as 20 Hz vs (40–220 Hz), 40 Hz vs (60–240 Hz), 60 Hz vs (85–310 Hz), 80 Hz vs (110–380 Hz), and 100 Hz vs (130–400 Hz) to obtain JNDs for each standard frequency value and to test for Weber's law.

Similarly, the experiment was repeated for discrimination of a low-frequency comparison stimulus from a high-frequency standard stimulus. The standard frequency values were 110, 220, 310, 380, and 400 Hz, while the comparison frequency was randomized from (100–10 Hz), (200–20 Hz), (285–60 Hz), (350–80 Hz), and (370–100 Hz) respectively for each of the standard frequency values. JNDs were calculated for each of the standard frequency values as explained before to test for Weber's law.

Statistical analysis

Repeated measures one-way ANOVA was used to test the significance of relationship between stimulation parameters and sensory detection thresholds in both rats and monkeys (Fig. 3h, 3i, 3j, 5g, 5h, 5i, and Supplementary Fig. 4c and 4f). To test whether JNDs were significantly linearly related to standard frequency in the sensory discrimination task, the linear regression test was used (Fig. 7b and 7d).

CRediT authorship contribution statement

Amol P. Yadav: Conceptualization, Methodology, Software, Investigation, Formal analysis, Funding acquisition, Supervision, Writing – original draft, Writing – review & editing. **Shuangyan Li:** Methodology, Investigation, Formal analysis, Writing – review & editing. **Max O. Krucoff:** Conceptualization, Methodology, Funding acquisition, Writing – review & editing. **Mikhail A. Lebedev:** Conceptualization, Writing – review & editing. **Muhammad M. Abd-El-Barr:** Methodology, Writing – review & editing. **Miguel A.L. Nicolelis:** Resources, Funding acquisition, Supervision, Writing – review & editing.

Declaration of competing interest

The authors declare no competing financial or non-financial interests.

Acknowledgements

We thank Gary Lehew for assistance with experimental setup, Tamara Phillips for assistance with monkey handling, Paul Thompson for assistance with primate task software, Laura Oliveira and Susan Halkiotis for technical assistance, and Joseph O'Doherty for comments on previous version of manuscript. This research was supported by Duke Institute for Brain Sciences Germinator Award and Duke Neurosurgery Research Support awarded to Amol P. Yadav, NIH R25 awarded to Max O. Krucoff, RSF grant 21-75-30024 awarded to Mikhail A. Lebedev, and Hartwell Foundation grant awarded to Miguel Nicolelis.

Appendix A. Supplementary data

Supplementary data to this article can be found online at https://doi.org/10.1016/j.brs.2021.04.024.

References

[1] Lebedev MA, Nicolelis MA. Brain-Machine interfaces: from basic science to neuroprostheses and neurorehabilitation. Physiol Rev 2017;97(2):767–837. https://doi.org/10.1152/physrev.00027.2016. PubMed PMID: 28275048.

[2] Krucoff MO, Rahimpour S, Slutzky MW, Edgerton VR, Turner DA. Enhancing nervous system recovery through neurobiologics, neural interface training, and neurorehabilitation. ARTN 584 Front Neurosci 2016;10. https://doi.org/10.3389/fnins.2016.00584. PubMed PMID: WOS:000390598100001.

[3] Bensmaia SJ, Miller LE. Restoring sensorimotor function through intracortical interfaces: progress and looming challenges. Nat Rev Neurosci 2014;15(5):313–25. https://doi.org/10.1038/nrn3724. PubMed PMID: 24739786.

[4] O'Doherty JE, Lebedev MA, Ifft PJ, Zhuang KZ, Shokur S, Bleuler H, Nicolelis MA. Active tactile exploration using a brain-machine-brain interface. Nature 2011;479(7372):228–31. https://doi.org/10.1038/nature10489. PubMed PMID: 21976021; PMCID: 3236080.

[5] Kim S, Callier T, Tabot GA, Gaunt RA, Tenore FV, Bensmaia SJ. Behavioral assessment of sensitivity to intracortical microstimulation of primate somatosensory cortex. 49. In: Proceedings of the national academy of Sciences of the United States of America. vol. 112; 2015. p. 15202–7. https://doi.org/10.1073/pnas.1509265112. PubMed PMID: 26504211; PMCID: 4679002.

[6] Tabot GA, Dammann JF, Berg JA, Tenore FV, Boback JL, Vogelstein RJ, Bensmaia SJ. Restoring the sense of touch with a prosthetic hand through a brain interface. P Natl Acad Sci USA 2013;110(45):18279–84. https://doi.org/10.1073/pnas.1221113110. PubMed PMID: WOS:000326550800062.

[7] Flesher SN, Collinger JL, Foldes ST, Weiss JM, Downey JE, Tyler-Kabara EC, Bensmaia SJ, Schwartz AB, Boninger ML, Gaunt RA. Intracortical microstimulation of human somatosensory cortex. Epub 2016/11/01 Sci Transl Med 2016;8(361):361ra141. https://doi.org/10.1126/scitranslmed.aaf8083. PubMed PMID: 27738096.

[8] Heming E, Sanden A, Kiss ZH. Designing a somatosensory neural prosthesis: percepts evoked by different patterns of thalamic stimulation. J Neural Eng 2010;7(6):064001. https://doi.org/10.1088/1741-2560/7/6/064001. PubMed PMID: 21084731.

[9] Swan BD, Gasperson LB, Krucoff MO, Grill WM, Turner DA. Sensory percepts induced by microwire array and DBS microstimulation in human sensory thalamus. Brain Stimul 2018;11(2):416–22. https://doi.org/10.1016/j.brs.2017.10.017. PubMed PMID: 29126946; PMCID: PMC5803348.

[10] Dadarlat MC, O'Doherty JE, Sabes PN. A learning-based approach to artificial sensory feedback leads to optimal integration. Epub 2014/11/25 Nat Neurosci 2015;18(1):138–44. https://doi.org/10.1038/nn.3883. PubMed PMID: 25420067; PMCID: PMC4282864.

[11] Strauss I, Valle G, Artoni F, D'Anna E, Granata G, Di Iorio R, Guiraud D, Stieglitz T, Rossini PM, Raspopovic S, Petrini FM, Micera S. Characterization of multi-channel intraneural stimulation in transradial amputees. Epub 2019/12/19 Sci Rep 2019;9(1):19258. https://doi.org/10.1038/s41598-019-55591-z. PubMed PMID: 31848384; PMCID: PMC6917705.

[12] Petrini FM, Valle G, Bumbasirevic M, Barberi F, Bortolotti D, Cvancara P, Hiairrassary A, Mijovic P, Sverrisson AO, Pedrocchi A, Divoux JL, Popovic I, Lechler K, Mijovic B, Guiraud D, Stieglitz T, Alexandersson A, Micera S, Lesic A, Raspopovic S. Enhancing functional abilities and cognitive integration of the lower limb prosthesis. Epub 2019/10/04 Sci Transl Med 2019;11(512). https://doi.org/10.1126/scitranslmed.aav8939. PubMed PMID: 31578244.

[13] Petrini FM, Bumbasirevic M, Valle G, Ilic V, Mijovic P, Cvancara P, Barberi F, Katic N, Bortolotti D, Andreu D, Lechler K, Lesic A, Mazic S, Mijovic B, Guiraud D, Stieglitz T, Alexandersson A, Micera S, Raspopovic S. Sensory feedback restoration in leg amputees improves walking speed, metabolic cost and phantom pain. Epub 2019/09/11 Nat Med 2019;25(9):1356–63. https://doi.org/10.1038/s41591-019-0567-3. PubMed PMID: 31501600.

[14] Yadav AP, Li D, Nicolelis MAL. A brain to spine interface for transferring artificial sensory information. Epub 2020/01/23 Sci Rep 2020;10(1):900. https://doi.org/10.1038/s41598-020-57617-3. PubMed PMID: 31964948.

[15] Bellanca RU, Lee GH, Vogel K, Ahrens J, Kroeker R, Thom JP, Worlein JM. A simple alopecia scoring system for use in colony management of laboratory-housed primates. Epub 2014/02/28 J Med Primatol 2014;43(3):153–61. https://doi.org/10.1111/jmp.12107. PubMed PMID: 24571509; PMCID: PMC4438708.

[16] Ekman G. Weber law and related functions. J Psychol 1959;47(2):343–52. https://doi.org/10.1080/00223980.1959.9916336. PubMed PMID: WOS: A1959CAK1200020.

[17] Bjanes DA, Moritz CT. A robust encoding scheme for delivering artificial sensory information via direct brain stimulation. Epub 2019/08/24 IEEE Trans Neural Syst Rehabil Eng 2019;27(10):1994–2004. https://doi.org/10.1109/TNSRE.2019.2936739. PubMed PMID: 31443035.

[18] Merrill DR, Bikson M, Jefferys JG. Electrical stimulation of excitable tissue: design of efficacious and safe protocols. Epub 2005/01/22 J Neurosci Methods 2005;141(2):171–98. https://doi.org/10.1016/j.jneumeth.2004.10.020. PubMed PMID: 15661300.

[19] Cogan SF, Ludwig KA, Welle CG, Takmakov P. Tissue damage thresholds during therapeutic electrical stimulation. Epub 2016/01/23 J Neural Eng 2016;13(2):021001. https://doi.org/10.1088/1741-2560/13/2/021001. PubMed PMID: 26792176; PMCID: PMC5386002.

[20] Romo R, Hernandez A, Zainos A, Brody CD, Lemus L. Sensing without touching: psychophysical performance based on cortical microstimulation. Neuron 2000;26(1):273–8. PubMed PMID: 10798410.

[21] O'Doherty JE, Shokur S, Medina LE, Lebedev MA, Nicolelis MAL. Creating a neuroprosthesis for active tactile exploration of textures. 43. In: Proceedings of the national academy of Sciences of the United States of America. vol. 116; 2019. p. 21821–7. https://doi.org/10.1073/pnas.1908008116. Epub 2019/10/09, PubMed PMID: 31591224; PMCID: PMC6815176.

[22] Callier T, Brantly NW, Caravelli A, Bensmaia SJ. The frequency of cortical microstimulation shapes artificial touch. 2. In: Proceedings of the national academy of Sciences of the United States of America. vol. 117; 2020. p. 1191–200. https://doi.org/10.1073/pnas.1916453117. Epub 2019/12/28, PubMed PMID: 31879342; PMCID: PMC6969512.

[23] Holsheimer J, Barolat G. Spinal geometry and paresthesia coverage in spinal cord stimulation. Neuromodulation : J. Int. Neuromod. Soc. 1998;1(3):129–36. https://doi.org/10.1111/j.1525-1403.1998.tb00006.x. PubMed PMID: 22150980.

[24] Barolat G, Massaro F, He J, Zeme S, Ketcik B. Mapping of sensory responses to epidural stimulation of the intraspinal neural structures in man. Epub 1993/02/01 J Neurosurg 1993;78(2):233–9. https://doi.org/10.3171/jns.1993.78.2.0233. PubMed PMID: 8421206.

[25] Holsheimer J, Buitenweg JR. Review: bioelectrical mechanisms in spinal cord stimulation. discussion 70 Neuromodulation : J. Int. Neuromod. Soc. 2015;18(3):161–70. https://doi.org/10.1111/ner.12279. PubMed PMID: 25832787.

[26] North RB, Sieracki JM, Fowler KR, Alvarez B, Cutchis PN. Patient-interactive, microprocessor-controlled neurological stimulation system. Epub 1998/10/01 Neuromodulation : J. Int. Neuromod. Soc. 1998;1(4):185–93. https://doi.org/10.1111/j.1525-1403.1998.tb00015.x. PubMed PMID: 22151030.

[27] Holsheimer J. Which neuronal elements are activated directly by spinal cord stimulation. Epub 2002/01/01 Neuromodulation : J. Int. Neuromod. Soc. 2002;5(1):25–31. https://doi.org/10.1046/j.1525-1403.2002._2005.x. PubMed PMID: 22151778.

[28] Yadav AP, Nicolelis MAL. Electrical stimulation of the dorsal columns of the spinal cord for Parkinson's disease. Mov Disord 2017;32(6):820–32. https://doi.org/10.1002/mds.27033. PubMed PMID: 28497877.

[29] Yadav AP, Fuentes R, Zhang H, Vinholo T, Wang CH, Freire MA, Nicolelis MA. Chronic spinal cord electrical stimulation protects against 6-hydroxydopamine lesions. Sci Rep 2014;4:3839. https://doi.org/10.1038/srep03839. PubMed PMID: 24452435; PMCID: 3899601.

[30] Yadav AP, Borda E, Nicolelis MA. Closed loop spinal cord stimulation restores locomotion and desynchronizes corticostriatal beta oscillations [abstract]. Mov Disord 2018;33.

[31] Pais-Vieira M, Yadav AP, Moreira D, Guggenmos D, Santos A, Lebedev M, Nicolelis MA. A closed loop brain-machine interface for epilepsy control using dorsal column electrical stimulation. Sci Rep 2016;6:32814. https://doi.org/10.1038/srep32814. PubMed PMID: 27605389; PMCID: PMC5015048.

[32] Hanson TL, Omarsson B, O'Doherty JE, Peikon ID, Lebedev MA, Nicolelis MA. High-side digitally current controlled biphasic bipolar microstimulator. Epub 2012/02/14 IEEE Trans Neural Syst Rehabil Eng 2012;20(3):331–40. https://doi.org/10.1109/TNSRE.2012.2187219. PubMed PMID: 22328184; PMCID: PMC3502026.

[33] Pais-Vieira M, Chiuffa G, Lebedev M, Yadav A, Nicolelis MA. Building an organic computing device with multiple interconnected brains. Sci Rep 2015;5:11869. https://doi.org/10.1038/srep11869. PubMed PMID: 26158615; PMCID: 4497302.

[34] Rahimpour S, Gaztanaga W, Yadav AP, Chang SJ, Krucoff MO, Cajigas I, et al. Freezing of Gait in Parkinson's Disease: Invasive and Noninvasive Neuromodulation. Neuromodulation: Technol Neural Interfac 2020. https://doi.org/10.1111/ner.13347. Pubmed PMID: 33368872.